Pergamon

PII: S0045-7949(96)00014-4

*Computers & Structures* Vol. 61, No. 1, pp. 43–54, 1996

0045-7949/96 $15.00 + 0.00

# A TWO-LEVEL ITERATIVE FEM TECHNIQUE FOR RIGOROUS SOLUTION OF NON-LINEAR INTERACTION PROBLEMS UNDER LARGE DEFORMATIONS

**K. El-Sawy** and **I. D. Moore**
Department of Civil Engineering, University of Western Ontario, London, Ontario, Canada N6A 5B9

(*Received* 2 *March* 1995)

**Abstract**—Various problems arising in applied mechanics involve interaction between two bodies having separation, bonding, re-bonding and slip at the interface. Simple FEM models assume one of the two extremes, "bonded interface" or "smooth interface". Alternative spring models have been developed to model slip, shear strength and dilation. These models are applicable for small deformations and coincident nodes at the interface. The paper describes a rigorous solution for the problem which does not sacrifice the simplicity of the FEM approach. In this study the deformations are assumed to be large enough to change the geometry of the problem and the interface is assumed to be a frictional adhesive one with a *coulomb* failure criterion. The technique examines the interaction of two bodies, namely the *slave* and *master* bodies. It simulates frictional slip, separation, bonding and re-bonding of the slave body with respect to the master allowing for large deformations and non-matching nodes at the interface. The proposed solution is iterative where two levels of iterations are used. The first iteration procedure is used to satisfy equilibrium and to deal with the geometrical non-linearity, while the second is used to satisfy the interaction conditions at the interface. The proposed technique is illustrated with a number of test problems of varying complexity. These demonstrate that the approach performs well for problems involving interaction of two bodies under large deformations. Copyright © 1996 Elsevier Science Ltd.

## DEFINITION OF THE PROBLEM

The problem of interaction between two bodies subjected to large deformations is a challenging one. Where deformations are small, the assumption of "node to node" interaction (Fig. 1a) is valid and the solution is straightforward while in the case of large deformations the "node to surface" interaction (Fig. 1b) or "surface to surface" interaction [1] has to be modelled which makes the problem more difficult. In this study, the choice of "node to surface" interaction is made as it is more appropriate and general. Furthermore, interface behaviour, such as separation, bonding, re-bonding and slippage must be modelled.

A simple rigorous approach to solve these problems is developed. This work is an extension of Katona's formulation for the case of small deformations [2]. The features of the rigorous approach are its simplicity and compatibility with FEM solution subroutines. It also avoids the calculation of flexibility matrices for the interacting bodies and the associated problem of rigid body movement [3].

The two interacting bodies are named the *master* and the *slave* bodies. Each body is discretized using nodes and isoparametric elements. The master interface is discretized into a series of interface elements. Each interface element is defined by its nodal connectivity. The order of these nodes is chosen to define the correct outward normal to the master interface. The "node to surface" contact is identified by a *slave node S* and a *master interface element*. The projection of the slave node $S$ on the master interface is defined by point $S^*$. The angle between the outward normal to the master interface at point $S^*$ and the $X$-axis is denoted $\theta$ and its positive direction is anticlockwise. The displacements in the global $X$–$Y$ directions are denoted $u_x$ and $u_y$, while the displacments in the local normal and tangential directions are denoted $u_n$ and $u_t$. Figure 2 shows an $m$-noded master interface element, a slave node $S$ and the two coordinate systems.

## SOME USEFUL RELATIONS

The relations between the incremental Cartesian displacements $\Delta u_x$ and $\Delta u_y$ and the incremental normal and tangential displacements $\Delta u_n$ and $\Delta u_t$ are as follows:

$$\begin{Bmatrix} \Delta u_n \\ \Delta u_t \end{Bmatrix} = \begin{bmatrix} c & s \\ -s & c \end{bmatrix} \begin{Bmatrix} \Delta u_x \\ \Delta u_y \end{Bmatrix}, \tag{1}$$

$$\begin{Bmatrix} \Delta u_x \\ \Delta u_y \end{Bmatrix} = \begin{bmatrix} c & -s \\ s & c \end{bmatrix} \begin{Bmatrix} \Delta u_n \\ \Delta u_t \end{Bmatrix}, \tag{2}$$

where $s=\sin(\theta)$ and $c=\cos(\theta)$.

Some relations can also be developed between incremental displacements at the slave node projection $S^*$ and an $m$-noded master interface element defined by $m$ nodes and the incremental displacements at these nodes.

$$\begin{Bmatrix} \Delta u_{xS^*} \\ \Delta u_{yS^*} \end{Bmatrix} = \begin{bmatrix} N_1 & 0 & \cdots & \cdots & N_m & 0 \\ 0 & N_1 & \cdots & \cdots & 0 & N_m \end{bmatrix} \begin{Bmatrix} \Delta u_{x1} \\ \Delta u_{y1} \\ \vdots \\ \vdots \\ \Delta u_{xm} \\ \Delta u_{ym} \end{Bmatrix}, \tag{3}$$

$$\begin{Bmatrix} \Delta u_{nS^*} \\ \Delta u_{tS^*} \end{Bmatrix} = \begin{bmatrix} cN_1 & sN_1 & \cdots & \cdots & -cN_m & sN_m \\ -sN_1 & cN_1 & \cdots & \cdots & -sN_m & cN_m \end{bmatrix} \begin{Bmatrix} \Delta u_{x1} \\ \Delta u_{y1} \\ \vdots \\ \vdots \\ \Delta u_{xm} \\ \Delta u_{ym} \end{Bmatrix}, \tag{4}$$

where $N_1$–$N_m$ are the master interface element shape functions defined at point $S^*$.

## GOVERNING EQUATIONS FOR THE TWO INTERACTING BODIES

The stiffness equations for the two interacting bodies are available using conventional techniques and can be written as

$$\begin{Bmatrix} \begin{Bmatrix} 0 \\ \Delta F_{si} \end{Bmatrix} \\ \begin{Bmatrix} 0 \\ \Delta F_{mi} \end{Bmatrix} \end{Bmatrix} + \begin{Bmatrix} \begin{Bmatrix} \Delta R_s \\ \Delta R_{si} \end{Bmatrix} \\ \begin{Bmatrix} \Delta R_m \\ \Delta R_{mi} \end{Bmatrix} \end{Bmatrix} = \begin{bmatrix} \mathbf{K}_s & 0 \\ 0 & \mathbf{K}_m \end{bmatrix} \begin{Bmatrix} \begin{Bmatrix} \Delta U_s \\ \Delta U_{si} \end{Bmatrix} \\ \begin{Bmatrix} \Delta U_m \\ \Delta U_{mi} \end{Bmatrix} \end{Bmatrix}, \tag{5}$$

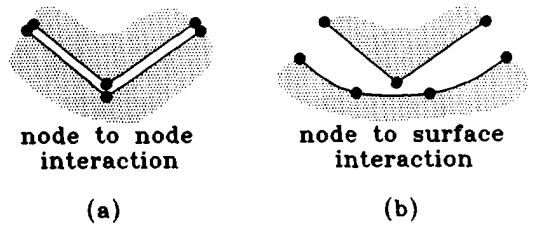


Fig. 1. Interaction types.

where:

$\Delta R_m, \Delta U_m$ are the master body incremental applied forces and displacements at non-interfacial nodes;

$\Delta R_s, \Delta U_s$ are the slave body incremental applied forces and displacements at non-interfacial nodes;

$\Delta R_{mi}, \Delta U_{mi}$ are the master body incremental applied forces and displacements at the interface nodes;

$\Delta R_{si}, \Delta U_{si}$ are the slave body incremental applied forces and displacements at the interface nodes;

$\Delta F_{mi}$ are the master body incremental interaction forces at the interface nodes;

$\Delta F_{si}$ are the slave body incremental interaction forces at the inteface nodes;

$\mathbf{K}_m$ is the tangent stiffness matrix of the master body;

$\mathbf{K}_s$ is the tangent stiffness matrix of the slave body.

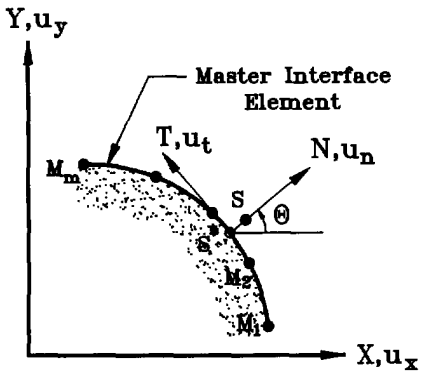


Fig. 2. System of coordinates.

There are unknowns on both sides of the equation. On the left-hand side there are the unknown incremental interaction forces, $\Delta F_{mi}$ and $\Delta F_{si}$, while all the displacements shown on the right-hand side are unknown. To solve this problem, extra constraint equations relating the two bodies' incremental displacements and incremental interaction forces will be developed to augment eqn (5).

### CONDENSATION OF THE STIFFNESS MATRICES TO THE INTERFACE

As the solution of the interaction problem is iterative, eqn (5) is condensed first to remove the degrees of freedom which are not concerned with the interaction problem and to reduce the computational effort. The condensed stiffness equations can be written as

$$\begin{Bmatrix} \Delta F_{si} \\ \Delta F_{mi} \end{Bmatrix} + \begin{Bmatrix} \Delta P_{si} \\ \Delta P_{mi} \end{Bmatrix} = \begin{bmatrix} \mathbf{K}_{si} & 0 \\ 0 & \mathbf{K}_{mi} \end{bmatrix} \begin{Bmatrix} \Delta U_{si} \\ \Delta U_{mi} \end{Bmatrix}, \quad (6)$$

where:

$\Delta P_{mi}$ are the condensed incremental forces at the master body interface nodes;
$\Delta P_{si}$ are the condensed incremental applied forces at the slave body interface nodes;
$\mathbf{K}_{mi}$ is the condensed tangent stiffness matrix of the master body;
$\mathbf{K}_{si}$ is the condensed tangent stiffness matrix of the slave body.

All the rotational degrees of freedom are condensed as the interaction problem concerns constraints on the nodal translations.

### TWO-LEVEL ITERATION TECHNIQUE

Before proceeding, it is useful to discuss the solution technique employed. As in many non-linear FE analyses, the load is applied in small increments (or steps) while iterations are performed to satisfy the equilibrium of the two bodies. In this study, these equilibrium iterations are also called the *major iterations*. This major iteration deals with any material or geometrical non-linearities.

A second iteration loop is also introduced into the interaction analysis. These iterations are designated the *minor iterations*. Within the minor iteration loop, a mode of interaction at each slave interface node is assumed, the constraint equations are formulated and a trial solution is obtained. A check for the validity of the assumed modes determines whether another trial is required.

### APPLICATION OF THE CONSTRAINT EQUATIONS TO THE GOVERNING EQUATIONS

As in a small deformation analysis featuring node–node interaction, the constraint equations either impose displacement compatibility or force equilibrium. The same concept applies for a large deformation analysis involving node–surface interaction. Compatibility and equilibrium equations are derived for each slave interface node $S$ and the $m$-noded master interface element with which it interacts. The displacement compatibility constraint equations at the $i$th minor iteration take the following form:

$$\{f_1\}_{2\times 1} = [[a] \mid [b] \mid [d]]_{2\times(4+2m)} \begin{bmatrix} \Delta u^i_{xS} \\ \Delta u^i_{yS} \\ \text{----} \\ \Delta u^i_{x_1} \\ \Delta u^i_{y_1} \\ \vdots \\ \vdots \\ \Delta u^i_{x_m} \\ \Delta u^i_{y_m} \\ \text{----} \\ \Delta F_{nS} \\ \Delta F_{tS} \end{bmatrix}_{(4+2m)\times 1} . \quad (7)$$

To impose force equilibrium, constraint equations are developed for the $i$th minor iteration:

$$-\begin{bmatrix} \Delta F_{xS} \\ \Delta F_{yS} \\ \text{- - - -} \\ \Delta F_{x_1} \\ \Delta F_{y_1} \\ \vdots \\ \vdots \\ \Delta F_{x_m} \\ \Delta F_{y_m} \end{bmatrix}_{(2+2m)\times 1} = \begin{bmatrix} [a]^T \\ \text{- - -} \\ [b]^T \end{bmatrix}_{(2+2m)\times 2} \begin{Bmatrix} \Delta F^i_{nS} \\ \Delta F^i_{tS} \end{Bmatrix}_{2\times 1}, \quad (8)$$

where:

$\Delta u^i_{xS}$ is the incremental slave node displacement in the $X$-direction;

$\Delta u^i_{yS}$ is the incremental slave node displacement in the $Y$-direction;

$\Delta u^i_{x_m}$ is the incremental displacement of the $m$th node of the master element in the $X$-direction;

$\Delta u^i_{y_m}$ is the incremental displacement of the $m$th node of the master element in the $Y$-direction;

$\Delta F^i_{nS}$ is the incremental slave node force normal to the master surface;

$\Delta F^i_{tS}$ is the incremental slave node force tangential to the master surface;

$\Delta F^i_{xS}$ is the incremental slave node force in the $X$-direction;

$\Delta F^i_{yS}$ is the incremental slave node force in the $Y$-direction;

$\Delta F^i_{x_m}$ is the incremental force in the $X$-direction for the $m$th node of the master element;

$\Delta F^i_{y_m}$ is the incremental force in the $Y$-direction for the $m$th node of the master element;

$\mathbf{a}, \mathbf{b}, \mathbf{d}$ are constraint matrix sub-matrices;

$\mathbf{f}_i$ is a constant vector.

Equation (7) is calculated, for each slave node, and added to the governing system of equations [eqn (6)]. Each side of eqn (8) is added to the corresponding side of eqn (6) to get rid of the unknown incremental interaction forces. The new system of equations is written as

$$\begin{Bmatrix} \Delta P_{si} \\ \Delta P_{mi} \\ 0 \end{Bmatrix} + \{F\} = \begin{bmatrix} \mathbf{K}_{si} & 0 & \mathbf{A}^T \\ 0 & \mathbf{K}_{mi} & \mathbf{B}^T \\ \mathbf{A} & \mathbf{B} & \mathbf{D} \end{bmatrix} \begin{Bmatrix} \Delta U_{si} \\ \Delta U_{mi} \\ \{\Delta F_{ns}\} \\ \{\Delta F_{ts}\} \end{Bmatrix}, \quad (9)$$

where

$\mathbf{F}$ are additional load vectors;

$\mathbf{A}, \mathbf{B}, \mathbf{D}$ are constraint matrices depending on the modes of interaction;

$\Delta F_{ns}$ are incremental normal interaction forces at the slave interface nodes

$\Delta F_{ts}$ are incremental tangential interaction forces at the slave interface nodes.

This places all the unknowns into one side of the equation facilitating the solution. For each slave node and its interacting master interface element a constraint matrix $[c]$ and a load vector $\{f\}$ are defined. The constraint matrix is expressed as

$$[c] = \begin{bmatrix} 0 & 0 & [a]^T \\ 0 & 0 & [b]^T \\ [a] & [b] & [d] \end{bmatrix}. \quad (10)$$

These constraint matrices and load vectors augment the system of governing equations yielding eqn (9).

## CONSTRAINT MATRICES AND LOAD VECTORS FOR DIFFERENT INTERACTION MODES

A number of different interaction conditions (or modes) are possible for the slave interface nodes. Three different conditions, namely *free*, *sliding* and *fixed* modes, are examined. For each mode, the constraint matrix $[c]$ and load vector $\{f\}$ at the slave node are derived.

### *Free mode of interaction*

For this mode, the slave node $S$ separates from the master interface and the "total" interaction forces diminish to zero. In other words, the applied "incremental" interaction forces at the slave node $S$, at the $k$th major iteration and the $i$th minor iteration, should cancel out the "total" interaction forces at the previously converged $(k-1)$th major iteration. This can be expressed as

$$\begin{Bmatrix} \Delta F^i_{nS} \\ \Delta F^i_{tS} \end{Bmatrix} = \begin{Bmatrix} -F^{k-1}_{nS} \\ -F^{k-1}_{tS} \end{Bmatrix}, \quad (11)$$

and

$$\begin{Bmatrix} \Delta F^i_{xS} \\ \Delta F^i_{yS} \end{Bmatrix} = \begin{bmatrix} c & -s \\ s & c \end{bmatrix} \begin{Bmatrix} -F^{k-1}_{nS} \\ -F^{k-1}_{tS} \end{Bmatrix} = \begin{Bmatrix} -cF^{k-1}_{nS} + sF^{k-1}_{tS} \\ -sF^{k-1}_{nS} - cF^{k-1}_{tS} \end{Bmatrix}, \quad (12)$$

where $F^{k-1}_{nS}$, $F^{k-1}_{tS}$ are the total normal and tangential interaction forces at slave node $S$ at the previously converged major iteration (i.e. the $(k-1)$th major iteration). In eqns (11) and (12) superscript $i$ stands for the $i$th minor iteration while superscript $k-1$ stands for the $(k-1)$th major iteration.

For this mode the slave incremental interaction forces are known *a priori* and they are used to derive the incremental interaction forces for the master interface nodes by the method of virtual work [3]. The incremental forces at the nodes of an $m$-noded master interface element are the nodal forces equivalent to point loads equal and opposite to the incremental applied loads at the slave node $S$ and can be given by

$$\begin{Bmatrix} \Delta F^i_{x_1} \\ \Delta F^i_{y_1} \\ \vdots \\ \vdots \\ \Delta F^i_{x_m} \\ \Delta F^i_{y_m} \end{Bmatrix} = \begin{bmatrix} N_1 & 0 \\ 0 & N_1 \\ \vdots & \vdots \\ \vdots & \vdots \\ N_m & 0 \\ 0 & N_m \end{bmatrix} \begin{Bmatrix} \Delta F^{k-1}_{xS} \\ \Delta F^{k-1}_{yS} \end{Bmatrix} = \begin{bmatrix} cN_1 & -sN_1 \\ sN_1 & cN_1 \\ \vdots & \vdots \\ \vdots & \vdots \\ cN_m & -sN_m \\ sN_m & cN_m \end{bmatrix} \begin{Bmatrix} \Delta F^{k-1}_{nS} \\ \Delta F^{k-1}_{tS} \end{Bmatrix}. \quad (13)$$

The corresponding constraint matrix $[c]$ and load vector $\{f\}$ are defined in Table 1.

*Fixed mode of interaction*

When the slave node $S$ attaches to the master interface, the displacement compatibility equation for node $S$ and its projection $S^*$ on the master surface element should be imposed into the governing system of equations. At the $k$th major and $i$th minor iteration the compatibility equation can be written as

$$\begin{Bmatrix} g^{k-1} \\ g^{k-1}\left(\dfrac{\Delta u_{tS^*}^{i-1} - \Delta u_{tS}^{i-1}}{\Delta u_{nS^*}^{i-1} - \Delta u_{nS}^{i-1}}\right) \end{Bmatrix} = \begin{Bmatrix} \Delta u_{nS^*}^{i} \\ \Delta u_{tS^*}^{i} \end{Bmatrix} - \begin{Bmatrix} \Delta u_{nS}^{i} \\ \Delta u_{tS}^{i} \end{Bmatrix}, \quad (14)$$

where:

$g^{k-1}$ is the normal gap between the slave node and the master surface element at the $(k-1)$th major iteration;

$\Delta u_{nS}^{i}$ is the incremental displacement at slave node $S$ normal to the master interface at the $i$th minor iteration;

$\Delta u_{tS}^{i}$ is the incremental displacement at slave node $S$ tangent to the master interface at the $i$th minor iteration;

$\Delta u_{nS^*}^{i}$ is the incremental displacement at point $S^*$ normal to the master interface at the $i$th minor iteration;

$\Delta u_{tS^*}^{i}$ is the incremental displacement at point $S^*$ tangent to the master interface at the $i$th minor iteration.

For the tangential displacements it is assumed that the slave node $S$ and its projection $S^*$ are moving in the same direction as that calculated in the previous minor iteration.

The terms in the right-hand side of eqn (14) can be written as

$$\begin{Bmatrix} \Delta u_{nS^*}^{i} \\ \Delta u_{tS^*}^{i} \end{Bmatrix} = \begin{bmatrix} cN_1 & sN_1 & \cdots & \cdots & cN_m & sN_m \\ -sN_1 & cN_1 & \cdots & \cdots & -sN_m & cN_m \end{bmatrix} \begin{Bmatrix} \Delta u_{x1}^{i} \\ \Delta u_{y1}^{i} \\ \vdots \\ \vdots \\ \Delta u_{xm}^{i} \\ \Delta u_{ym}^{i} \end{Bmatrix}, \quad (15)$$

$$\begin{Bmatrix} \Delta u_{nS}^{i} \\ \Delta u_{tS}^{i} \end{Bmatrix} = \begin{Bmatrix} c\Delta u_{xS}^{i} + s\Delta u_{yS}^{i} \\ -s\Delta u_{xS}^{i} + c\Delta u_{yS}^{i} \end{Bmatrix}. \quad (16)$$

Now the equilibrium equations for the interface forces have to be imposed as well. Using the concept of virtual work, the incremental forces at the master interface element nodes can be related to the slave node incremental interaction forces. This relation is written as

$$-\begin{Bmatrix} \Delta F_{x1}^{i} \\ \Delta F_{y1}^{i} \\ \vdots \\ \vdots \\ \Delta F_{xm}^{i} \\ \Delta F_{ym}^{i} \end{Bmatrix} = \begin{bmatrix} N_1 & 0 \\ 0 & N_1 \\ \vdots & \vdots \\ \vdots & \vdots \\ N_m & 0 \\ 0 & N_m \end{bmatrix} \begin{Bmatrix} \Delta F_{xS}^{i} \\ \Delta F_{yS}^{i} \end{Bmatrix} = \begin{bmatrix} cN_1 & -sN_1 \\ sN_1 & cN_1 \\ \vdots & \vdots \\ \vdots & \vdots \\ cN_m & -sN_m \\ sN_m & cN_m \end{bmatrix} \begin{Bmatrix} \Delta F_{nS}^{i} \\ \Delta F_{tS}^{i} \end{Bmatrix}. \quad (17)$$

Equation (17) directly defines matrix $[b]^T$, in eqn (8), while matrix $[a]^T$ transforms terms from the normal and tangential system of coordinates to the Cartesian one. The constraint matrix $[c]$ and load vector $\{f\}$ for the "fixed" mode of interaction are defined in Table 1.

*Sliding interaction mode*

When the slave node $S$ slides along the master interface, compatibility is prescribed for the displacements normal to the master interface. The compatibility equation can be written as

$$\Delta u_{nS^*}^{i} - \Delta u_{nS}^{i} = g^{k-1}, \quad (18)$$

Table 1. Surface element constraint matrix [$C$] and load vector[$f$] for three modes of interaction during the $i$th minor (mode assumption convergence) iteration within the $k$th major iteration

| State | $\Delta u^i_{cS}$ | $\Delta u^i_{tS}$ | $\Delta u^i_{c1}$ | $\Delta u^i_{t1}$ | ··· | ··· | $\Delta u^i_{cm}$ | $\Delta u^i_{tm}$ | $\Delta F^i_{nS}$ | $\Delta F^i_{tS}$ | Load |
|---|---|---|---|---|---|---|---|---|---|---|---|
| Fixed | 0 | 0 | 0 | 0 | 0 | 0 | 0 | 0 | $-c$ | $s$ | 0 |
| | 0 | 0 | 0 | 0 | 0 | 0 | 0 | 0 | $-s$ | $-c$ | 0 |
| | 0 | 0 | 0 | 0 | 0 | 0 | 0 | 0 | $cN_1$ | $-sN_1$ | 0 |
| | 0 | 0 | 0 | 0 | 0 | 0 | 0 | 0 | $sN_1$ | $cN_1$ | 0 |
| | 0 | 0 | 0 | 0 | 0 | 0 | 0 | 0 | : | : | 0 |
| | 0 | 0 | 0 | 0 | 0 | 0 | 0 | 0 | : | : | 0 |
| | 0 | 0 | 0 | 0 | 0 | 0 | 0 | 0 | $cN_m$ | $-sN_m$ | 0 |
| | 0 | 0 | 0 | 0 | 0 | 0 | 0 | 0 | $sN_m$ | $cN_m$ | 0 |
| | $-c$ | $-s$ | $cN_1$ | $sN_1$ | ··· | ··· | $cN_m$ | $sN_m$ | 0 | 0 | $g^{k-1}$ |
| | $s$ | $-c$ | $-sN_1$ | $cN_1$ | ··· | ··· | $-sN_m$ | $cN_m$ | 0 | 0 | $g^{k-1}\left(\frac{\Delta u^{i-1}_{tS\bullet} - \Delta u^{i-1}_{tS}}{\Delta u^{i-1}_{nS\bullet} - \Delta u^{i-1}_{nS}}\right)$ |
| Sliding | 0 | 0 | 0 | 0 | 0 | 0 | 0 | 0 | $-c$ | 0 | $-s(T^i_{max} - F^{k-1}_{tS})$ |
| | 0 | 0 | 0 | 0 | 0 | 0 | 0 | 0 | $-s$ | 0 | $c(T^i_{max} - F^{k-1}_{tS})$ |
| | 0 | 0 | 0 | 0 | 0 | 0 | 0 | 0 | $cN_1$ | 0 | $sN_1(T^i_{max} - F^{k-1}_{tS})$ |
| | 0 | 0 | 0 | 0 | 0 | 0 | 0 | 0 | $sN_1$ | 0 | $-cN_1(T^i_{max} - F^{k-1}_{tS})$ |
| | 0 | 0 | 0 | 0 | 0 | 0 | 0 | 0 | : | : | : |
| | 0 | 0 | 0 | 0 | 0 | 0 | 0 | 0 | : | : | : |
| | 0 | 0 | 0 | 0 | 0 | 0 | 0 | 0 | $cN_m$ | 0 | $sN_m(T^i_{max} - F^{k-1}_{tS})$ |
| | 0 | 0 | 0 | 0 | 0 | 0 | 0 | 0 | $sN_m$ | 0 | $-cN_m(T^i_{max} - F^{k-1}_{tS})$ |
| | $-c$ | $-s$ | $cN_1$ | $sN_1$ | ··· | ··· | $cN_m$ | $sN_m$ | 0 | 0 | $g^{k-1}$ |
| | 0 | 0 | 0 | 0 | ··· | ··· | 0 | 0 | 0 | 1 | $T^i_{max} - F^{k-1}_{tS}$ |
| Free | 0 | 0 | 0 | 0 | 0 | 0 | 0 | 0 | 0 | 0 | $-cF^{k-1}_{nS} + sF^{k-1}_{tS}$ |
| | 0 | 0 | 0 | 0 | 0 | 0 | 0 | 0 | 0 | 0 | $-sF^{k-1}_{nS} - cF^{k-1}_{tS}$ |
| | 0 | 0 | 0 | 0 | 0 | 0 | 0 | 0 | 0 | 0 | $N_1(cF^{k-1}_{nS} - sF^{k-1}_{tS})$ |
| | 0 | 0 | 0 | 0 | 0 | 0 | 0 | 0 | 0 | 0 | $N_1(sF^{k-1}_{nS} + cF^{k-1}_{tS})$ |
| | 0 | 0 | 0 | 0 | 0 | 0 | 0 | 0 | : | : | : |
| | 0 | 0 | 0 | 0 | 0 | 0 | 0 | 0 | : | : | : |
| | 0 | 0 | 0 | 0 | 0 | 0 | 0 | 0 | 0 | 0 | $N_m(cF^{k-1}_{nS} - sF^{k-1}_{tS})$ |
| | 0 | 0 | 0 | 0 | 0 | 0 | 0 | 0 | 0 | 0 | $N_m(sF^{k-1}_{nS} + cF^{k-1}_{tS})$ |
| | 0 | 0 | 0 | 0 | ··· | ··· | 0 | 0 | 1 | 0 | $-F^{k-1}_{nS}$ |
| | 0 | 0 | 0 | 0 | ··· | ··· | 0 | 0 | 0 | 1 | $-F^{k-1}_{tS}$ |

$N_i$ the $i$th shape function of the master line element defined at the point of projection of the slave node on the element;
$\theta$ angle between the outward normal to the master surface element and the $X$-axis where $s$ and $c$ are defined as $s = \sin(\theta)$ and $c = \cos(\theta)$;
$T^i_{max}$ the total maximum shear force between the slave node and the interacting master element at the $k$th major and $i$th minor iteration;
$g^{k-1}$ the gap between the slave node and the master surface element at the $(k-1)$th major iteration; it is positive if there is no penetration and negative otherwise;
$F^{k-1}_{nS}$ the normal component of the total interaction force at the slave node at the $(k-1)$th major iteration; it is positive if in the same direction as the outward normal to the master surface element;
$F^{k-1}_{tS}$ the tangential component of the total interaction force at the slave node at the $(k-1)$th major iteration.

or

$$[cN_1 \quad sN_1 \quad \cdots \quad \cdots \quad cN_m \quad sN_m] \begin{Bmatrix} \Delta u^i_{x1} \\ \Delta u^i_{y1} \\ \vdots \\ \vdots \\ \Delta u^i_{xm} \\ \Delta u^i_{ym} \end{Bmatrix} - (c\Delta u^i_{xS} + s\Delta^i_{yS}) = g^{k-1}. \tag{19}$$

Another condition for slip is that the total tangential force at the slave node should be equal to the maximum frictional force available. The maximum frictional force is initially unknown, and firstly has to be estimated according to the previously converged major iteration, and then to be modified (or updated) throughout the minor iterations. At the $i$th minor iteration the maximum frictional force is defined by

$$T_{\max} = (|F^{k-1}_{nS} + \Delta F^i_{nS}|\tan(\phi) + c)\operatorname{sgn}(F^{k-1}_{tS} + \Delta F^i_{tS}), \tag{20}$$

and the condition for the sliding state can be expressed as

$$\Delta F^i_{tS} = T^i_{\max} - F^{k-1}_{tS}. \tag{21}$$

Like interaction for the "free" mode, the incremental tangential slave node force is known and will generate a load vector at both the slave node and the interacting master interface element nodes. On the other hand, the normal incremental force at the slave node is unknown and a relationship between this force and the master slave nodes can be found (as before in the fixed mode). The corresponding constraint matrix and load vector are defined in Table 1.

## FORMULATION OF THE RESIDUAL FORCE VECTOR

Two methods are used to calculate the residual load vector $\{\Delta R^k\}$ shown on the left-hand side of eqn (5). In both methods the residual load vector is defined as

$$\{\Delta P^k\} = \{R^k\} - \{F^k\}, \tag{22}$$

where $\{R^k\}$ is the total applied force vector at the $k$th major iteration and $\{F^k\}$ is the nodal force vector which is equivalent (in the virtual work sense) to the current stresses at the $k$th major iteration.

The two methods differ in how the total force vector $\{R^k\}$ is defined at the interfacial nodes. The first method accumulates the incremental interaction forces at the slave nodes throughout the major iterations to get the total forces at these nodes. The total forces at the master interface nodes are calculated from the total forces at the slave interface nodes using the concept of virtual work.

The second method equates the total interaction forces at the slave interfacial nodes to the equivalent nodal forces due to the current stress state. In other words, the residual forces at the interfacial slave nodes become zero. The total forces at the master interface nodes are calculated as before in the first method.

The two methods are used to study the effect of accumulating the incremental interaction forces (the first method). In general, the second method for calculating the residual force vector promoted superior convergence, but the final results were more or less the same.

## CRITERIA FOR SELECTING NEW MODES DURING MINOR ITERATIONS

A comprehensive set of physical criteria to test the validity of an assumed mode is shown in Table 2. The table shows a decision matrix used for checking the mode in the previous minor iteration to determine the new most probable mode.

It is worth mentioning that in the third row in Table 2, an assumed free mode is correct if the normal gap is greater than zero, otherwise the new mode is assumed fixed. This does not imply a sliding mode cannot be reached from a free mode, it simply implies a sliding state must be reached by an iterative path; free–fixed–sliding. For the special case of smooth interface, one can go directly from free to sliding mode.

## CONSTRAINT EQUATIONS FOR RESTRAINED INTERFACE NODES

The equation for each restrained degree of freedom is deleted from the system leaving only the displacements of the unrestrained degrees of freedom to be determined. However, for restrained slave nodes, while the degree of freedom for one direction is restrained and the corresponding equation is removed, the equations corresponding to the normal and tangential interaction forces at this slave node are not removed from the system of equations. These

Table 2. Decision matrix for selecting new interaction mode during minor (mode assumption convergence) iteration within the $k$th major (equilibrium) iteration

| Iteration | | Current minor iteration $i$ for slave node $S$ | | |
|---|---|---|---|---|
| | Fixed mode | Sliding mode | Free mode | |
| Previous minor iteration $(i-1)$ for slave node $S$ | Fixed mode | $F^i_{nS} > 0$ and $\lvert F^i_{tS}\rvert < T^i_{max}$ | $F^i_{nS} > 0$ and $\lvert F^i_{tS}\rvert > T^i_{max}$ | $F^i_{nS} \leqslant 0$ |
| | Sliding mode | $F^i_{nS} > 0$ and $T^i_{max}(\Delta u^i_{tS^*} - \Delta u^i_{tS}) < 0$ | $F^i_{nS} > 0$ and $T^i_{max}(\Delta u^i_{tS^*} - \Delta u^i_{tS}) > 0$ | $F^i_{nS} \leqslant 0$ |
| | Free mode | $g < 0$ | Not applicable | $g > 0$ |

$T^i_{max}$ the total maximum shear force between the slave node and the interacting master element at the $k$th major iteration and the $i$th minor iteration;
$F^i_{nS}$ the normal component of the total interaction force at the slave node at the $k$th major iteration and the $i$th minor iteration; it is positive if in the same direction as the outward normal to the master surface element;
$F^i_{tS}$ the tangential component of the total interaction force at the slave node at the $k$th major iteration and the $i$th minor iteration;
$\Delta F^i_{tS}$ the tangential component of the incremental interaction force between the slave node and the interacting master element at the $k$th increment and the $i$th minor iteration;
$\Delta u^i_{tS}$ the tangential component of the slave node incremental displacement at the $k$th major iteration and the $i$th minor iteration;
$\Delta u^i_{tS^*}$ the tangential component of the incremental displacement of the point of projection of the slave node on the master surface element at the $k$th major iteration and the $i$th minor iteration;
$g$ the gap between the slave node and the master interface at the $k$th major iteration and the $i$th minor iteration; it is negative if the slave node penetrates into the master surface element.

equations for the interaction forces are required to satisfy force equilibrium at the interface.

## TEST PROBLEMS

To examine the effectiveness of the proposed method of analysis, several different test problems are examined. The problems have been chosen to check different aspects of the method. In all the analyses, the structural elements used are those of Surana [4] and the continuum elements are 8-noded isoparametric elements. The expected interacting slave nodes are chosen and the expected interacting master surface is discretized by interface elements compatible with the discretization of the master body at the interface. In all the test problems, convergence is achieved through an adequate number of major iterations, and one minor iteration is used unless otherwise noted.

### *Problem of a beam with one pinned end and the other sliding on a rough surface*

The problem, shown in Fig. 3, is chosen for its simplicity and to check the proposed method against the analytical solution which is easily derived. It also demonstrates the ability of the method to detect "fixed" and "sliding" modes, and the applicability of the method when one of the individual interacting bodies is prone to have rotational rigid-body movements. In this case, the initial modes of interaction (sliding or fixed) should be assumed *a priori*, otherwise a singular system of equations is produced. The beam is modelled using one 5-noded structural element. The beam length $L$ and material properties $EA$ and $EI$ are shown in Fig. 3. The free end of the beam is considered a slave node and the rigid surface is modelled using an imaginary 5-noded interface element attached to five restrained nodes. The friction angle $\phi$ between the beam and the rough surface is 30°. The sliding end of the beam is subjected to a horizontal load $P$ which is increased till a maximum value of $P = 0.25$ is reached. This load is then released until $P$ reaches 0.0. Figure 3 shows

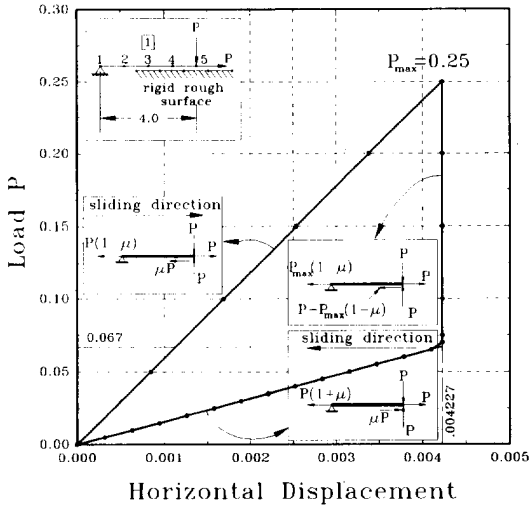


Fig. 3. Load–displacement response of a beam with one end pinned and the other sliding on a rough surface ($EA = 100$, $EI = 100/12$, $L = 4.0$, $\phi = 30$, $\mu = \tan\phi$).

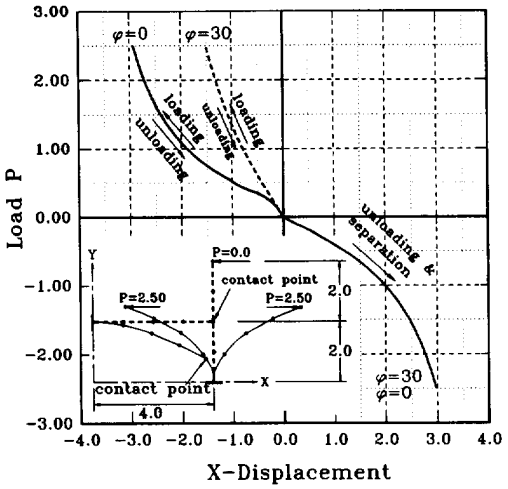


Fig. 4. Load–displacement response for a vertical cantilever contacting and separating from another horizontal one ($EA = 100$, $EI = 100/12$, $\Delta P = 0.05$, $\phi = 0$, 30).

all the data used in the analysis and also the resulting load–displacement relationship for the sliding end of the beam. It is shown that the loaded end of the beam slides in the direction of loading as the applied load increases to the maximum load $P = 0.25$. When the load decreases, the loaded end remains fixed to the rough surface until the limiting value $P = 0.067$, after which it slides in a direction opposite to that of the applied load due to the axial strain energy stored along the beam length. The numerical solution matches the analytical solution.

*Problem of a vertical cantilever contacting and separating from another horizontal one*

This simple problem, shown in Fig. 4, demonstrates the ability of the formulation to trace sliding and separation under large deformations. Each cantilever is modelled using a 5-noded structural element. The material properties and the dimensions of both cantilevers are shown in Fig. 4. The vertical cantilever surface is considered the master interface while the end of the horizontal cantilever is chosen to be the slave node. The load $P$ is applied in equal increments of $\Delta P = 0.05$. Two cases are considered, the rough interface with $\phi = 30^\circ$ and the smooth one with $\phi = 0^\circ$. The load–displacement response of the loaded end of the vertical cantilever is shown. The deformed shapes at load levels $P = 2.5$ and $-2.5$ for the case of $\phi = 0^\circ$ are also shown in the figure.

For the case of $\phi = 0^\circ$, the effect of the horizontal cantilever on the behaviour is pronounced at low load levels. Once the slave node slides along the master interface and the horizontal cantilever deforms, its stiffness in the direction normal to the deformed vertical cantilever decreases and its effect on the final deformation is negligible. This is not the case for $\phi = 30^\circ$, as full contact between the two cantilevers is maintained without slip, and displacements are substantially reduced.

*Problem of a long vertical cantilever contacting another distant shorter one*

Both the previous problems show bodies initially in contact. The contact is maintained at one node which is easy to trace and visualize. The third problem deals with two bodies initially separate, so that a contact surface is formed after load is applied. The two cantilevers have identical materials and are modelled using 5-noded structural elements. The long cantilever is modelled using five structural elements and is chosen to be the master body with its surface defined along the cantilever length. The short cantilever is modelled using three structural elements and its nodes are chosen to be the slave nodes. The case of smooth interface $\phi = 0^\circ$ is considered.

The problem dimensions, material properties and model discretization are shown in Fig. 5. The load–displacement response at the loaded end of the long cantilever is shown as well as the deformed shapes at load levels $M = 3.5$ and 5.0. At load level $M = 3.5$, there is only one point of contact between the cantilevers. At the higher load level $M = 5.0$, a contact surface had developed on which slip occurs.

*Problem of a cantilever contacting a rigid circular surface*

A more complicated problem of a cantilever bending onto a rigid circular surface is considered in Fig. 6. The cantilever is considered the slave body and is modelled using five 5-noded structural elements. The smooth rigid circular surface is considered the master surface and is modelled using six 5-noded imaginary interface elements attached to 25 restrained nodes. The material properties of the cantilever and dimensions of the problem are shown in Fig. 6. The deformed shape is illustrated at load

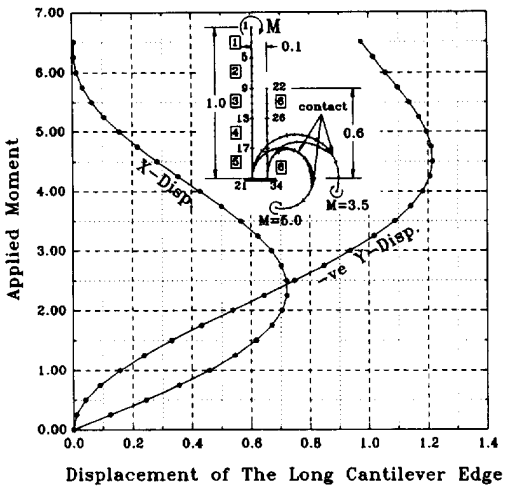


Fig. 5. Load–displacement response of the loaded end of a vertical cantilever contacting another distant shorter one ($EI = 1.0$, $EA = 12 \times 10^4$, $\Delta M = 0.05$, $\phi = 0.0$).

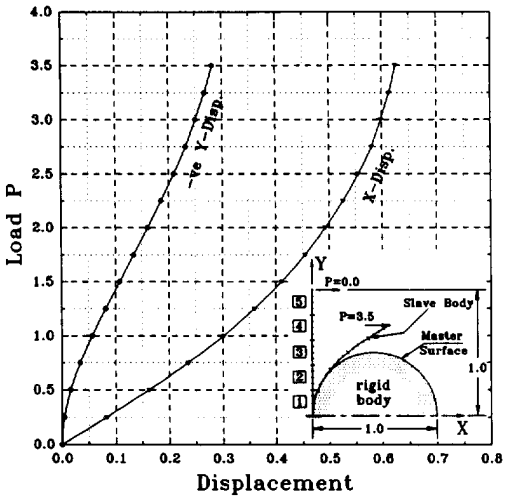


Fig. 6. Load–displacement response of the loaded end of a vertical cantilever contacting a rigid circular surface ($EI = 1.0$, $EA = 1.2 \times 10^7$, $\phi = 0.0$, $\Delta P = 0.005$).

$P = 3.5$ and the load–displacement response at the cantilever loaded end is shown. It is shown that as the applied load increases, the length of the contact surface increases and the free length of the cantilever decreases. This increases the stiffness of the cantilever and consequently decreases the rate of change of displacements.

*Problem of a cantilever resting against an elastic body*

The final problem is presented to demonstrate certain capabilities and the limitations of the interaction analysis in more detail. The cantilever is modelled using twelve 3-noded structural elements while the elastic body is modelled using 8-noded isoparametric continuum elements. All the dimensions and material properties (i.e. Young's modulus $E$ and Poisson's ratio $\nu$) are shown in Fig. 7. The cantilever is considered the master body with its surface defined along its length, while the elastic body nodes at the cantilever interface are considered the slave nodes. The case of a smooth interface is considered.

Trials with different sizes of load increment and different numbers of major and minor iterations are considered. The results are show in Figs 8–10. We can draw some conclusions from the solution of this problem:

(1) As in all incremental non-linear analyses, the size of the load increment may affect the accuracy of the results. Figure 8 shows that for load increments 0.01 and 0.02, the solution is indistinguishable which

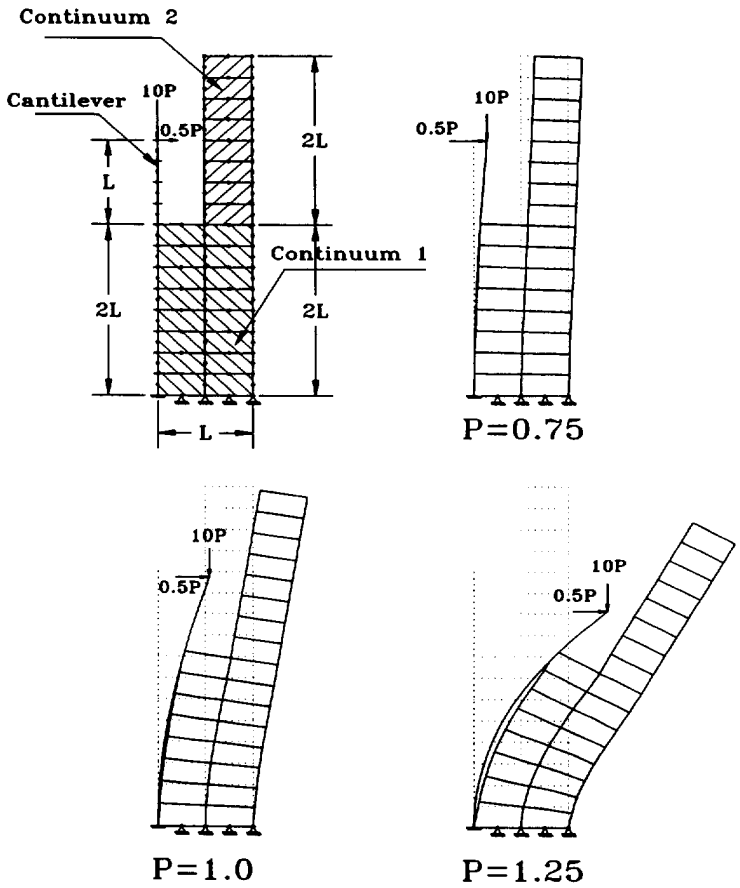


Fig. 7. A cantilever supported on an elastic body ($EI = 1.0$, $EA = 10^4$, $E_1 = 50.0$, $\nu_1 = 0.3$, $E_2 = 100.0$, $\nu_2 = 0.3$).

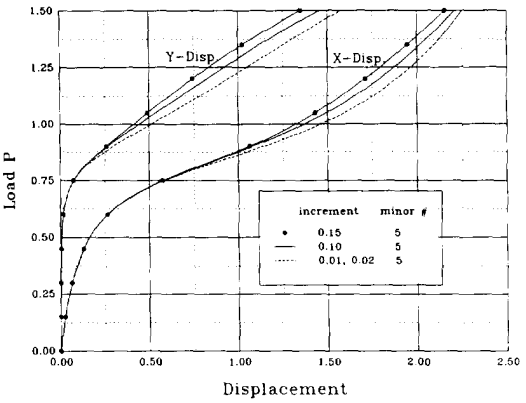


Fig. 8. Effect of the load increment size.

implies convergence to the correct numerical solution. Decreased accuracy of the solutions is also clear for the load increments 0.10 and 0.15, although there is numerical convergence. Decreased accuracy is not due to inappropriate modelling of the interface behaviour, but it is due to the fact that accurate material modelling in the updated Lagrangian formulation requires small load increments.

(2) The bigger the number of major (equilibrium) iterations the smoother the load–deflection behaviour. This result is because a decrease in residual force accelerates convergence to the correct interaction modes (Fig. 9). This can be seen from the slope discontinuities in the load–deflection curve obtained using one major iteration instead of five. Increasing the maximum number of minor iterations from five to 10 had no effect on the solution since convergence occurred in less than five iterations.

(3) Figure 10 gives results for alternatively 1, 2 and 5 minor iterations in the case of a large load increment, 0.15. For 1 and 2 minor iterations, no mode convergence is achieved at high load levels ($P > 0.95$). When five minor iterations are used, the solution is closer to that obtained using a small load increment. This demonstrates the advantage of using multiple minor interations which ensures convergence for solutions obtained using large load increments for which significant changes in interaction modes may occur.

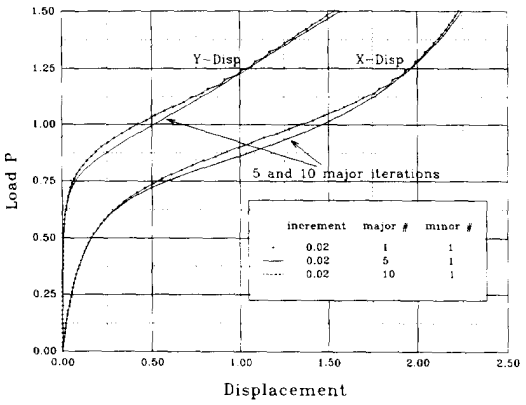


Fig. 9. Effect of number of equilibrium iterations.

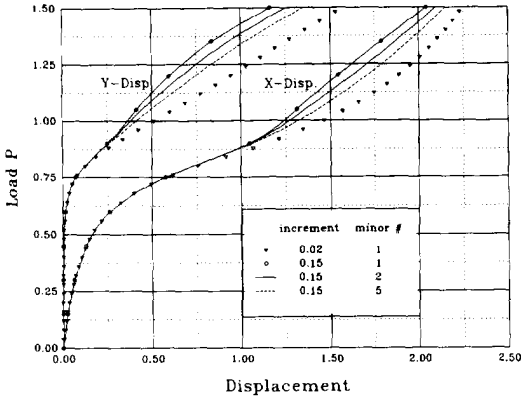


Fig. 10. Effect of number of minor iterations.

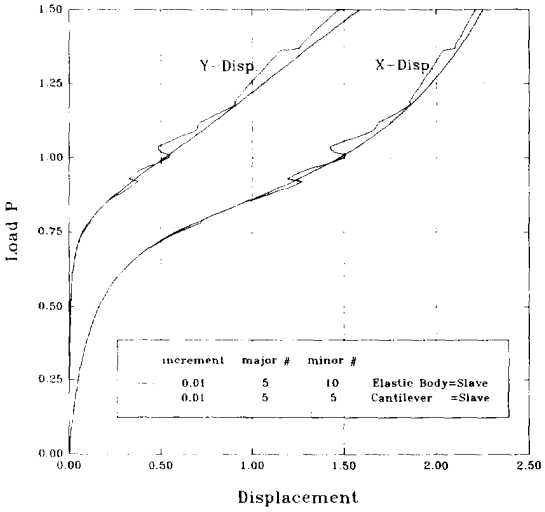


Fig. 11. Effect of the change of the master and slave roles.

The choice of the slave nodes and the master surface needs careful consideration as it may affect the results. To illustrate this point, two cases are considered where master and slave bodies are interchanged. The first case is that examined before, while the second case involves slave nodes along the cantilever length and the master surface defined along the continuum boundary.

Figure 11 shows the load–displacement response at the tip of the cantilever for the two different definitions of master and slave bodies. In the second case, a sudden change in the behaviour is noticed once each new slave node starts to interact with the master surface. Points such as the corner of an elastic solid are best treated as slave nodes, so they can steadily traverse the surface of the other body.

## CONCLUSIONS

Some final conclusions may be drawn from this study:

(1) The method is applicable to a very wide range of applications with interaction involving large deformations.

(2) The method is applicable when one or both interacting bodies are prone to rigid body movements.

(3) A study was conducted to examine the effect of various numerical parameters (e.g. increment size and number of major and minor iterations). This study showed that using a small number of minor iterations, in cases where significant mode changes occur or when large increment size is used, may cause the solution to depart from the true one.

(4) Under some circumstances, like those where it is difficult to distinguish between the free and fixed modes, no mode convergence is achieved and the minor iterations oscillate between two interaction states (open and closed interface). The same behaviour is reported by Katona [2] in his study of small deformations.

(5) In some cases, the choice of the master interface and the interacting slave nodes may affect the solution. Careful consideration should be given to surface and nodal compatibility when defining master and slave boundaries.

(6) The method can also be applied for multi-interacting bodies (although this is not shown here). In that case, the master interface would consist of a number of separate discretized interfaces, from which the correct interface element would be selected for each slave node.

*Acknowledgements*—Support for the research was provided through research and equipment grants from the Natural Sciences and Engineering Research Council of Canada.

## REFERENCES

1. K. J. Bathe and A. Chaudhary, On finite element analysis of large deformation contact problems. In: *Unification of Finite Element Methods* (Edited by H. Kardesuncer), Chap. 5, pp. 123–147. Elsevier, North-Holland (1984).
2. M. G. Katona, A simple contact–friction interface element with applications to buried culverts. *Int. J. numer. analyt. Meth. Geomech.* **7**, 371–384 (1983).
3. J. K. Kodikara and I. D. Moore, A general interaction analysis for large deformations. *Int. J. Numer. Meth. Eng.* **36**, 2863–2876 (1993).
4. K. S. Surana, Geometrically non-linear formulation for two-dimensional curved beam element. *Comput. Struct.* **17**, 105–114 (1983).